

- [4] a) G. Wulff, S. Gladow, B. Kühneweg, S. Krieger, presented at the 5th SPSP-Int. Conference in Osaka, Japan **1994**. See: G. Wulff, S. Gladow, B. Kühneweg, S. Krieger, *Macromol. Symp.* **1996**, 101, 355; b) S. Gladow, Dissertation, Universität Düsseldorf, **1994**.
- [5] G. Wulff, U. Zweering, S. Gladow, *Polym. Prepr. Am. Chem. Soc. Div. Polym. Chem.* **1996**, 37, 448.
- [6] T. Nakano, Y. Okamoto, D. Y. Sogah, S. Zheng, *Macromolecules* **1995**, 28, 8705–8706.
- [7] a) D. Sogah, S. Zheng, T. Nakano, *Polym. Prepr. Am. Chem. Soc. Div. Polym. Chem.* **1996**, 37, 442–443; b) S. Zheng, D. Y. Sogah, *Polym. Prepr. Am. Chem. Soc. Div. Polym. Chem.* **1997**, 38, 60–61; c) S. Zheng, D. Y. Sogah, *Tetrahedron* **1997**, 53, 15469–15485; D. Y. Sogah, S. Zheng, *Polym. Prepr. Am. Chem. Soc. Div. Polym. Chem.* **1999**, 40, 540–541.
- [8] Synthesis of the monocycle **C2** with $R = C(C_6H_5)_3$, $E = CH_3$: Under inert conditions THF (700 mL) (dried over BuLi) was condensed onto triphenylmethane (10.5 g, 42 mmol). At -84°C the mixture was stirred with BuLi (25 mL, 40 mmol) for 12 h. Subsequently, **M** (5.5 g, 8.5 mmol) in THF (16 mL) was slowly added in measured quantities over 100 min using a perfusor. After the addition, the mixture was stirred for 8 h. It was then stirred with CH_3I (10 mL) for a further 4 h. After concentration at 40°C the mixture was examined by ^1H NMR spectroscopy, and the major component **C2** purified by chromatography.
- [9] A. Matussek, Dissertation, Universität Düsseldorf, **1999**.
- [10] Hydrolysis of the monocycles: Compound **C** (1 g) in MeOH (1.4 L) was heated with concentrated H_2SO_4 (420 mL) under reflux for 120 h. After addition of H_2O (700 mL), the mixture was extracted four times with diethyl ether. The organic phase was washed with saturated $NaHCO_3$ solution until it was neutral, then washed with H_2O , and concentrated after drying with Na_2SO_4 . The compound was purified by chromatography. Yield **C_h** ~ 30 –60%, **B_h** ~ 30 %, **T_h** ~ 43 %, **P_h** ~ 75 %.
- [11] Crystal structure data for **C2**·hexane^[13].
- [12] Crystal structure data for **B2**:^[13] Crystals from $CHCl_3$ /pentane; $C_{98}H_{94}O_{12}$, $M_r = 1463.73$, orthorhombic, space group $P2_12_12_1$ (no. 19), $a = 15.106(3)$, $b = 17.289(4)$, $c = 38.611(8)$ Å, $V = 10084(3)$ Å³, 100 K, $Z = 4$, $\rho_{\text{calc}} = 0.96$ g cm⁻³, $\mu = 0.063$ mm⁻¹, crystal size $0.35 \times 0.25 \times 0.18$ mm, Nonius KappaCCD diffractometer, MoK_{α} radiation, $1.05 < \theta < 27.50^\circ$, 53982 measured reflections, 21803 independent, and 12130 with $I > 2\sigma(I)$, programs SHELXS-97 and SHELXL-97; both programs are from G. M. Sheldrick, Universität Göttingen, **1997**; 993 parameters, $R1 = 0.083$, $wR2$ (all data) = 0.259, $(\Delta/\sigma)_{\text{max}} = 0.001$, H atoms riding, max/min residual electron density 0.796/–0.366 e Å⁻³.
- [13] Crystallographic data (excluding structure factors) for the structures reported in this paper have been deposited with the Cambridge Crystallographic Data Centre as supplementary publication no. CCDC-139662 (**C2**) and CCDC-139663 (**B2**). Copies of the data can be obtained free of charge on application to CCDC, 12 Union Road, Cambridge CB21 1EZ, UK (fax: (+44) 1223-336-033; e-mail: deposit@ccdc.cam.ac.uk).
- [14] Y. Okamoto, H. Mohri, T. Nakano, K. Hatada, *J. Am. Chem. Soc.* **1989**, 111, 5952.
- [15] G. Wulff, U. Zweering, *Chem. Eur. J.* **1999**, 5, 1898–1904.

Bicyclo[3.2.1]DNA: On the Structural and Energetic Role of the Furanose Subunit in Complementary Strand Recognition of DNA**

Bernhard M. Keller and Christian J. Leumann*

Dedicated to Professor Richard Neidlein on the occasion of his 70th birthday

The nucleic acids (DNA, RNA) are the molecular “master-tapes” of all genetic information in living systems. In a cell, protein-controlled DNA replication proceeds with high efficiency, high speed, and high fidelity. Only a limited number of mutations, responsible for sequence evolution of DNA and thus the evolution of species, are admitted. The functional properties of DNA and RNA, which have outperformed alternative complementary base-pairing systems during molecular evolution,^[1] therefore demand structure–function correlation studies.^[2]

Experimental investigations showed that removal of the central ring in the nucleoside units, as in the acyclic DNA analogues glycerol-DNA,^[3] 1,2-*seco*-DNA^[4] (Figure 1), and

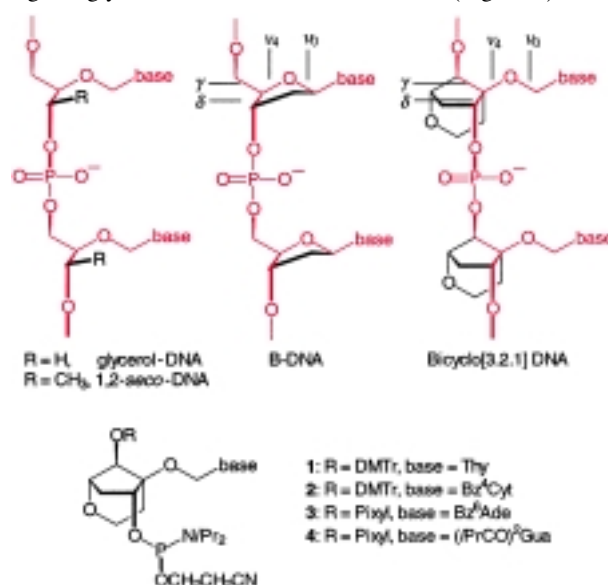


Figure 1. Above: Section of the chemical structures of glycerol-DNA, 1,2-*seco*-DNA, natural B-DNA, and bicyclo[3.2.1]DNA. The commonly shared structural features in the sugar-phosphate backbones of the four systems are drawn in red. The sugar- and backbone torsion angles ν_0 , ν_4 , γ , and δ differ in their conformational freedom in the three pairing systems. Essentially, no rotational restriction around the four torsion angles ν_0 , ν_4 , γ , and δ occurs in glycerol- and 1,2-*seco*-DNA. In B-DNA, the torsion angles δ , ν_0 , and ν_4 , are restricted by the furanose ring. In bicyclo[3.2.1]DNA, the backbone torsion angles γ and δ are frozen in a geometry similar to that observed in B-DNA duplexes, while the endocyclic torsion angles ν_0 , ν_4 are conformationally flexible. Below: The building blocks for the synthesis of bicyclo[3.2.1]oligonucleotides. DMTr = (4,4'-dimethoxy)triphenylmethyl, Pixyl = 9'-phenyl xanthenyl, Bz = benzoyl.

[*] Prof. C. J. Leumann, Dipl.-Chem. B. M. Keller
Department of Chemistry and Biochemistry
University of Bern
Freiestrasse 3, 3012 Bern (Switzerland)
Fax: + (41) 31-631-3422
E-mail: leumann@ioc.unibe.ch

[**] Financial support by the Swiss National Science Foundation is gratefully acknowledged. B.M.K. thanks the Roche Science Foundation for a PhD stipendium.

related systems,^[5] leads to incompetent complementary base-pairing systems, most likely because of the high entropic costs for conformational reorganization of the single strands upon duplex formation. On the other hand, investigations in the areas of antisense research^[6–12] and prebiotic chemistry^[13–16] give an increasing number of DNA-like base-pairing systems, based on cyclic nucleoside analogues, that show characteristic structural and functional properties.

From the supramolecular point of view, it remains an open question whether the connection between the bases and the phosphodiester backbone needs to be a ring system in order to obtain a base-pairing system which is sensitive to base mismatches and selective to strand orientation. We decided to address this question with the DNA analog bicyclo[3.2.1]-DNA. In this analogue, the phosphodiester backbone is preorganized in a B-DNA conformation, while the base is attached to the backbone via an acyclic linking unit.^[17] While we have already demonstrated that the pyrimidine-containing bicyclo[3.2.1]oligonucleotide forms duplexes with complementary DNA,^[18] we show here that bicyclo[3.2.1]DNA is, by itself, a selective base-pairing system.

The synthesis of the bicyclo[3.2.1]oligonucleotides started from the corresponding phosphoramidite building blocks **1–4** according to adapted protocols for solid-phase DNA synthesis and will be reported in detail elsewhere. In order to explore the base-pairing properties, a series of 10–20 nucleotide unit sequences were prepared and their integrity verified by ESI⁺ mass spectrometry (Table 1). For reasons of their synthesis, all bicyclo[3.2.1]oligonucleotides bear a natural deoxynucleotide unit at their 3' end (represented in bold type in Table 1).

To determine the relative differences in stability between duplexes in the bicyclo[3.2.1]DNA and the natural DNA series, UV-melting curve experiments were performed. With the exception of the adenine- and thymine-containing homodecamers, the bicyclo[3.2.1]oligonucleotides formed stable, antiparallel duplexes (Table 2). Their melting temperatures (T_m) were generally lower by 1.5–2.5 K per base pair compared to the natural oligonucleotides. Neglecting the energetic contribution of the terminal base pairs in the duplexes, this represents an average increase in the value of ΔG^0 of 0.7–0.8 kcal mol^{−1} per base pair (25 °C). The decrease in melting temperature for the bicyclo[3.2.1]DNA 15-mer

Table 1. Sequence and mass spectrometric data of the bicyclo[3.2.1]oligonucleotides used in this investigation.

bicyclo[3.2.1]oligonucleotides	ESI ⁺ -MS	
	calcd.	found
5'-AAAAAAAAAA-3'	3574.5	3574.0
5'-AAGAGAGGGAAGA-3'	4778.3	4777.8
5'-AGAGAGAGAGAAAAA-3'	5500.8	5500.1
5'-AAAGAAAAAGAGAGGGAAGA-3'	7379.1	7379.3
5'-TTTTTTTTTT-3'	3484.5	3482.1 ^[a]
5'-TCTTCCCTCTCTT-3'	4473.3	4474.6
5'-TTCTCTCCCTTCT-3'	4473.3	4474.6
5'-TCTTCCCCCTCTT-3'	4458.8	4459.5
5'-TTTTTCTCTCTCTT-3'	5210.8	5212.6 ^[a]
5'-TCTTCCCTCTCTTTTCTT-3'	6982.1	6980.2 ^[a]

[a] Determined by MALDI-TOF mass spectrometry.

duplex relative to the bicyclo[3.2.1]DNA 13-mer duplex (Entry 2 versus 3 in Table 2) is likely to arise due to the higher content of A-T base pairs in the former duplex and indicates a stronger energetic contribution of G-C base pairs to the duplex stability of bicyclo[3.2.1]DNA.

Strand association in bicyclo[3.2.1]DNA is selective to orientation: Duplexes were formed only between antiparallel complementary strands. A test for the formation of a parallel duplex between two parallel complementary bicyclo[3.2.1]-oligonucleotide 13-mers was negative (Entry 5, Table 2). Thus, the mode of strand association is controlled remotely by the geometry of the backbone unit. Furthermore, as in DNA, base mismatch is strongly discriminated in bicyclo[3.2.1]DNA. This is inferred from the observation that within a 13-mer duplex of bicyclo[3.2.1]DNA, an A-C mismatch in the center of the sequence completely forbids duplex formation (Entry 6, Table 2; compare with Entry 2 for the fully matched duplex).

Preliminary information on the structure of bicyclo[3.2.1]DNA duplexes was obtained from CD spectroscopy and molecular modeling. The CD spectrum of the antiparallel, complementary bicyclo[3.2.1]DNA 20-mer duplex (Entry 4, Table 2) is reminiscent of a Watson–Crick base-paired A-type double helix and different from that of the corresponding DNA duplex, which adopts a B-DNA conformation (Figure 2). This was unexpected, since the backbone torsion angle δ —which is mostly responsible for the conformational

Table 2. Melting points (T_m) from the UV melting curves (260 nm) of a series of DNA and the bicyclo[3.2.1]DNA duplexes of 10–20 base pairs.^[a]

Entry	Duplex	T_m [°C]	ΔT_m [K] ^[b]	$\Delta G^{25^\circ\text{C}}$ [kcal mol ^{−1}] ^[c]
1	5'-AAAAAAAAAA TTTTTTTTTT-5'	DNA [3.2.1]DNA	33 < 0	− 7.3 −
2	5'-AAGAGAGGGAAGA TTCTTCCCTTCT-5'	DNA [3.2.1]DNA	52.6 20.8	− 16.0 − 7.7
3	5'-AGAGAGAGAGAAAAA TCTCTCTCTTTTT-5'	DNA [3.2.1]DNA	54.9 18.4	− 17.1 − 6.6
4	5'-AGAAGGGAGAGAAAAAGAAA TCTTCCCTCTCTTTTCTTT-5'	DNA [3.2.1]DNA	61.9 30.6	− 25.2 − 11.2
5	5'-AAGAGAGGGAAGA 5'-TTCTTCCCTTCT	DNA [3.2.1]DNA	[d] < 0	− −
6	5'-AAGAGAGGGAAGA TTCTCCCCCTTCT-5'	DNA [3.2.1]DNA	[d] < 0	− −

[a] Experimental conditions: $c(\text{duplex}) = 2 \mu\text{M}$, in 10 mM Na cacodylate, 1 M NaCl, pH 7.0. [b] T_m difference between the DNA- and bicyclo[3.2.1]DNA-duplexes per base pair. [c] The values were obtained from curve fitting to the experimentally determined melting curve according to described procedures.^[18] [d] Not determined.

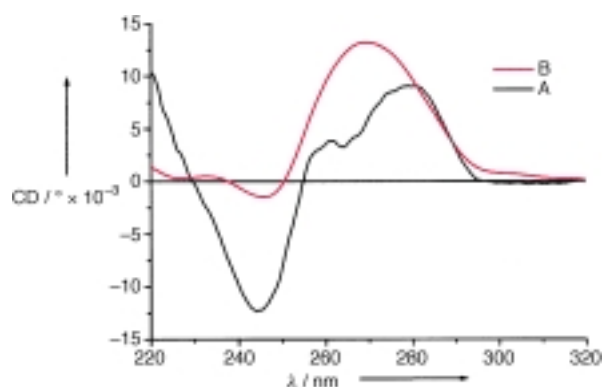


Figure 2. CD spectra of the DNA (A) and the bicyclo[3.2.1]DNA (B) duplexes which correspond to Entry 4 in Table 2 at 4 °C. Buffer conditions as indicated in Footnote [a], Table 2.

difference between the A- and B-DNA families—is restricted in bicyclo[3.2.1]DNA to values that are typical for B-DNA.

A molecular dynamics simulation of the bicyclo[3.2.1]DNA duplex corresponding to Entry 2 (Table 2) on a 200 ps trajectory with the initial structure in a B-DNA geometry revealed a double helical structure which roughly resembles that of a B-DNA double helix (Figure 3). No major differences, relative to DNA, are observed for the backbone torsion

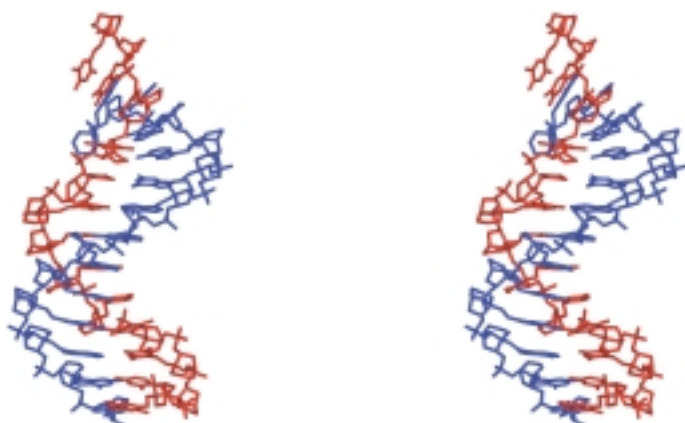


Figure 3. Stereoscopic view of the averaged structure of the last 50 ps of the 200 ps molecular dynamics simulation (Insight II/Discover) of the bicyclo[3.2.1]DNA duplex corresponding to Entry 2 in Table 2. For the simulation, the AMBER force field was used and a distance-dependent dielectric constant of $\epsilon = 4r$ was used to simulate an aqueous environment.

angles α – ζ . As expected, the linker region between the base and the backbone unit in bicyclo[3.2.1]DNA adopts a nearly perfect, extended conformation and thus differs from the corresponding structural unit in B-DNA. As a result, the base-stacking pattern in bicyclo[3.2.1]DNA becomes similar to A-DNA (Figure 4), which is in accord with the CD spectrum.

From the experimental results, the following conclusions with respect to the structural and energetic role of the furanose ring system in DNA can be drawn. 1) The entropic costs for duplex formation in a phosphodiester-based analogue of DNA, in which the bases are flexibly attached to the backbone, can be overcome if the backbone itself is restricted

conformationally. 2) Even without a ring system, which brings the nucleobases into a well defined orientation with respect to the backbone, strand orientation selectivity can be maintained. This is of interest with respect to the acyclic, peptide-based DNA analogue PNA, which only shows a very modest strand-orientation selectivity,^[19] and with respect to mixed, α/β -DNA duplexes, in which the preferred strand alignment is opposite (parallel) to that observed for β/β -DNA duplexes (antiparallel).^[20] 3) An increase in the translational and rotational degrees of freedom of a base pair in the center of the double helix does not lead to a loss in base-pairing selectivity.

Whatever the chemical determinants by which RNA and DNA became selected as a genetic material, phosphodiester-based systems devoid of a ring unit as a connector between the bases and backbone cannot collectively be excluded from the list of potential candidates in the selection process.

Received: February 16, 2000 [Z14713]

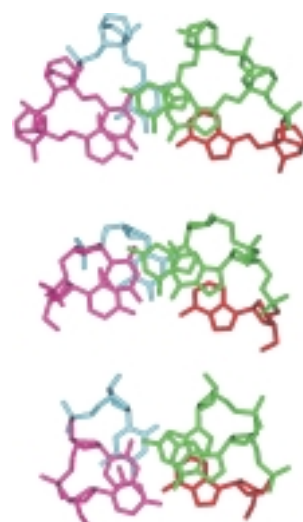


Figure 4. View along the helix axis of the central AGG-CCT unit in the modeled structure of the bicyclo[3.2.1]DNA 13-mer duplex (above), of canonical A-DNA (middle), and of canonical B-DNA (below). The similarity in the base-stacking pattern between A-DNA and the bicyclo[3.2.1]DNA is evident.

- [1] *The RNA World*, (Eds.: R. F. Gesteland, T. R. Cech, J. F. Atkins), 2nd ed., Cold Spring Harbor Laboratory Press, New York, **1999**.
- [2] A. Eschenmoser, M. Dobler, *Helv. Chim. Acta* **1992**, *75*, 218–259.
- [3] K. C. Schneider, S. A. Benner, *J. Am. Chem. Soc.* **1990**, *112*, 453–455.
- [4] L. Peng, H.-J. Roth, *Helv. Chim. Acta* **1997**, *80*, 1494–1512.
- [5] P. Nielsen, L. H. Dreier, J. Wengel, *Bioorg. Med. Chem.* **1995**, *3*, 19–28.
- [6] A. A. Koshkin, S. K. Singh, P. Nielsen, V. K. Rajwanshi, R. Kumar, M. Meldgaard, C. E. Olsen, J. Wengel, *Tetrahedron* **1998**, *54*, 3607–3630.
- [7] V. K. Rajwanshi, A. E. Hakansson, B. Dahl, J. Wengel, *Chem. Commun.* **1999**, 1395–1396.
- [8] C. Hendrix, H. Rosemeyer, I. Verheggen, F. Seela, A. Van Aerschot, P. Herdewijn, *Chem. Eur. J.* **1997**, *3*, 110–120.
- [9] Y. Maurinsh, H. Rosemeyer, R. Esnouf, A. Medvedovici, J. Wang, G. Ceulemans, E. Lescrinier, C. Hendrix, R. Busson, P. Sandra, F. Seela, A. Van Aerschot, P. Herdewijn, *Chem. Eur. J.* **1999**, *5*, 2139–2150.
- [10] M. Bolli, C. Litten, R. Schütz, C. Leumann, *Chem. Biol.* **1996**, *3*, 197–206.
- [11] M. Bolli, H. U. Trafelet, C. Leumann, *Nucleic Acids Res.* **1996**, *24*, 4660–4667.
- [12] R. Steffens, C. J. Leumann, *J. Am. Chem. Soc.* **1999**, *121*, 3249–3255.
- [13] M. Beier, F. Reck, T. Wagner, R. Krishnamurthy, A. Eschenmoser, *Science* **1999**, *283*, 699–703.
- [14] J. Hunziker, H.-J. Roth, M. Böhringer, A. Giger, U. Diederichsen, M. Göbel, R. Krishnan, B. Jaun, C. Leumann, A. Eschenmoser, *Helv. Chim. Acta* **1993**, *76*, 259–352.
- [15] O. Jungmann, H. Wippo, M. Stanek, H. K. Huynh, R. Krishnamurthy, A. Eschenmoser, *Org. Lett.* **1999**, *1*, 1527–1530.
- [16] S. Pitsch, R. Krishnamurthy, M. Bolli, S. Wendeborn, A. Holzner, M. Minton, C. Lesueur, I. Schönvogt, B. Jaun, A. Eschenmoser, *Helv. Chim. Acta* **1995**, *78*, 1621–1635.

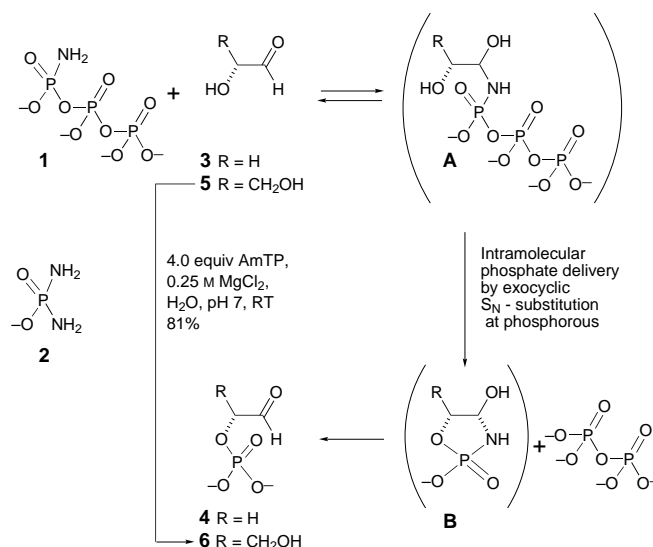
- [17] A different nucleoside analogue, based on similar design criteria, was presented in the literature (M. Marangoni, A. Van Aerschot, P. Augustyns, J. Rozenski, P. Herdewijn, *Nucleic Acids Res.* **1997**, *25*, 3034–3041). However, only the binding properties of oligonucleotides containing one such modification were described. Hence, no extrapolation to the properties of fully modified oligonucleotides is possible.
- [18] C. Epple, C. Leumann, *Chem. Biol.* **1998**, *5*, 209–216.
- [19] M. Egholm, O. Buchardt, L. Christensen, C. Behrens, S. M. Freier, D. A. Driver, R. H. Berg, S. K. Kim, B. Norden, P. E. Nielsen, *Nature* **1993**, *365*, 566–568.
- [20] F. Morvan, B. Rayner, J.-L. Imbach, M. Lee, J. A. Hartley, D.-K. Chang, J. W. Lown, *Nucleic Acids Res.* **1987**, *15*, 7027–7044.

Regioselective α -Phosphorylation of Aldoses in Aqueous Solution**

Ramanarayanan Krishnamurthy, Sreenivasulu Guntha, and Albert Eschenmoser*

In the context of studies on a potentially prebiotic chemistry of glycolaldehyde,^[3] we recently described an efficient conversion of this hydroxyaldehyde into its 2-phosphate in aqueous solution under very mild conditions (Scheme 1).^[1] The specific phosphorylation reagent in this process is amidotriphosphate (**1**, AmTP), a compound known to be formed by ammonolysis of cyclotriphosphate ("metatriphosphate") in aqueous solution.^[4] Significantly, cyclotriphosphate itself is not effective as a phosphorylation agent under the conditions where its ammonolysis product phosphorylates glycolaldehyde in essentially quantitative yields.^[1] The reason for this remarkable difference in reactivity is the specific capability of the amidotriphosphate to reversibly form a carbonyl addition product **A** with glycolaldehyde and to phosphorylate the α -hydroxyl group by intramolecular phosphate group delivery from **A** to the intermediate **B** which then undergoes hydrolysis to **4** (Scheme 1).

This mechanistic concept predicts that AmTP should have the potential to regioselectively phosphorylate the α -hydroxyl



Scheme 1. Regioselective intramolecular phosphorylation of glycolaldehyde ($R=H$) and D-glyceraldehyde ($R=CH_2OH$) by amidotriphosphate (**1**, AmTP).

groups of aldoses. Here we report that AmTP indeed reacts with glyceraldehyde, the tetrafuranses, and the four aldopentoses under mild conditions to form reaction products that are derived from intramolecular phosphate delivery to the hydroxyl group at the C-2 position of the sugar. We also found that a comparably efficient regioselective phosphorylation can be brought about with diamidophosphate (**2**, DAP)^[5] instead of AmTP as the phosphorylating reagent; in the case of aldofuranoses, there is even a preparative advantage with regard to product isolation.

D-glyceraldehyde (**5**), under the reaction conditions optimized for glycolaldehyde (0.025 M aqueous solution, 0.25 M $MgCl_2$, room temperature (RT), 5 days),^[1] reacts with the sodium salt of AmTP (4 equivalents, $pH \approx 7$) slowly but cleanly and with high regioselectivity, to give D-glyceraldehyde-2-phosphate (**6**; Scheme 1; 81 % yield after isolation by ion-exchange chromatography). No discernable glyceraldehyde-3-phosphate formation takes place according to 1H and ^{31}P NMR spectra of the reaction mixture.^[6]

In subjecting the two aldotetroses **7** and **10** to the same treatment, a similarly regioselective phosphorylation of the α -hydroxyl groups occurs, yet this time with a twist: the products are the 1,2-cyclophosphates **8** and **12**, isolated in yields of 87 % and 80 %, respectively. In the erythrose series (2,3-diol in *cis* configuration), about a tenth of the product material is the isomeric 2,3-cyclophosphate **9**, whereas in the threose series (2,3-diol in *trans* configuration) the 1,2-cyclophosphate is free of its 2,3-isomer (Scheme 2). D-ribose (**13**) with 4 equivalents of AmTP under similar conditions reacts more sluggishly and gives the furanosyl 1,2-cyclophosphate (**15**) besides the 2,3-cyclophosphates (**16a** and **16b**), with the latter in somewhat greater proportion than in the erythrose series (Scheme 2). Overall yields are lower (29 %), presumably due to trapping of intermediates in the pyranose form.^[7] According to exploratory experiments monitored by 1H and ^{31}P NMR spectroscopy, the other three pentoses behave similarly to ribose. The reaction of AmTP with hexoses was explored with

[*] Prof. Dr. A. Eschenmoser, Prof. Dr. R. Krishnamurthy, Dr. S. Guntha
Department of Chemistry and
The Skaggs Institute for Chemical Biology
The Scripps Research Institute
10550 North Torrey Pines Road, La Jolla, CA 92037 (USA)
Fax: (+1) 858-784-9573
E-mail: rkrishna@scripps.edu
and
Laboratorium für Organische Chemie
Eidgenössische Technische Hochschule
Universitätstrasse 16, 8092 Zürich (Switzerland)
Fax: (+41) 1-632-1043

[**] Chemistry of α -aminonitriles, Part 29. Part 28: Ref. [1], Part 27: Ref. [2]. This work was supported by the Skaggs Foundation. S.G. thanks the NASA NSCORT Exobiology program (La Jolla) for a postdoctoral fellowship.

Supporting information for this article is available on the WWW under <http://www.wiley-vch.de/home/angewandte/> or from R.K. (rkrishna@scripps.edu).